METHODS OF THE ATMOSPHERIC PARAMETERS DETERMINATIONS

T. A. Ryabchikova [a*]

[a] *Institute of Astronomy RAS, 119017, Pyatnitskaya str., 48, Moscow, Russia*

Different methods of fundamental parameters determinations – effective temperature ($T_{\rm eff}$), surface gravity (log g), metallicity ([M/H]), radius $R/R_{\odot}$, mass $M/M_{\odot}$, luminosity Ł for B to K stars are briefly described. They include both 'model-independent' methods such as total flux measurements + interferometry; asteroseismology ($T_{\rm eff}$, $R/R_{\odot}$, log g, $M/M_{\odot}$); and 'model-dependent' methods. The latter methods are based on the modelling of different observables such as photometric indexes, stellar spectra, stellar flux (Infra Red Flux method - IRFM).

A special attention is paid to spectroscopic methods. The first one is based on equivalent width measurements and excitation/ionization equilibrium. The second method is 'Spectroscopy Made Easy' (SME) package which fits the calculated spectrum to the observed one varying the global stellar parameters ($T_{\rm eff}$, log g, [M/H]) and parameters defining spectral line shape ($\xi_{\rm t}$, microturbulent and macroturbulent velocities). Although SME originally was developed for massive parameter determinations in F-G-K stars hosting planets, it is successfully working for B and A stars, in particular SME version that includes NLTE analysis.

Keywords: fundamental parameters – stars – photometry – interferometry – asteroseismology – spectroscopy

1. INTRODUCTION

Determination of fundamental stellar parameters is one of the most important tasks in astronomy. The accurate parameters and atmospheric abundances together with the star positions and kinematic properties allow us to constrain Galactic stellar populations and chemical evolution. I present a short review of the modern methods of stellar fundamental parameters determinations. These methods are either 'direct' – interferometry, asteroseismology, or 'model-dependent' such as photometry and spectroscopy.

* E-mail: ryabchik@inasan.ru

2. INTERFEROMENTRY

Stellar effective temperature $T_{\rm eff}$ may be derived from the Stefan-Boltzmann low: $T_{\rm eff} = \left(\frac{4f_{\rm bol}}{\sigma\theta^2_{\rm LD}}\right)^{1/4}$, if one knows the bolometric flux and stellar angular diameter. The modern observational interferometric technique allows us to measure angular diameters of relatively bright stars [2, 3] with an accuracy of 3 % and better. Linear diameters are estimated using known stellar parallaxes taken from Gaia DR2 catalogue [4], for example. The uncertainty of the linear radii is 3 – 5 %. Bolometric flux is derived by the integration of the observed photometric data calibrated in absolute units (see Fig. 1, taken from [3]).

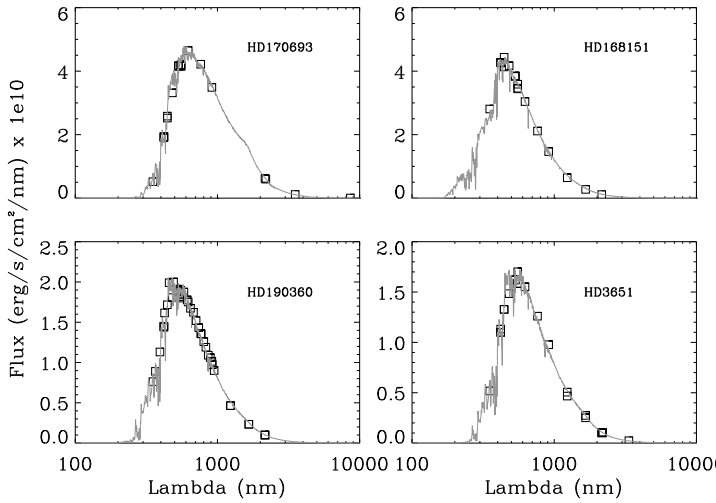

Fig. 1. Photometric energy distribution of four stars. Squares represent the photometric points and the grey curve represents the fitted spectrum. Copy of Fig.1 from [3].

Interferometry gives us direct stellar radii, effective temperatures and luminosities, although some modelling of the limb-darkening is applied. Stellar masses then are estimated from the evolutionary tracks, and surface gravites are derived from model-dependent masses and direct radii: $g/g_\odot = M/M_\odot(R/R_\odot)^{-2}$. A comparison of angular diameters derived with the different instruments shows an agreement within 10 % (see Fig.3 in [3]).

3. ASTEROSEISMOLOGY

Observations of the solar-like stellar pulsations privide a unique possibility for accurate mass, radius and surface gravity determinations. A short theory de-

scription is given in [5] and schematically represented in Fig. 2, which is taken from [5]. Large frequency separation between modes of the same angular degree ℓ and consecutive radial orders $n, n+1$ is proportional to stellar mass and radius: $\Delta\nu_0 \propto M^{1/2}R^{-3/2}$. This relation is valid for the Sun and stars with the solar-like oscillations. The second relation connects the frequency of the maximum power spectrum with the stellar fundamental parameters: $\nu_{max} \propto MR^{-2}T_{\rm eff}^{-1/2}$. Scaled to the solar values these two relations allow us to derive stellar mass and radius from the observed $\Delta\nu_0$ and ν_{max} if we know stellar effective temperature (direct method):

$$\frac{M}{M_\odot} \approx \left(\frac{\nu_{max}}{\nu_{max,\odot}}\right)^3 \left(\frac{\Delta\nu_0}{\Delta\nu_{0,\odot}}\right)^{-4} \left(\frac{T_{\rm eff}}{T_{\rm eff,\odot}}\right)^{3/2} \quad (1)$$

$$\frac{R}{R_\odot} \approx \left(\frac{\nu_{max}}{\nu_{max,\odot}}\right) \left(\frac{\Delta\nu_0}{\Delta\nu_{0,\odot}}\right)^{-2} \left(\frac{T_{\rm eff}}{T_{\rm eff,\odot}}\right)^{1/2} \quad (2)$$

One also may include models of stellar evolution for the masses and radii estimates calculating a grid of evolutionary tracks in a range of metallicities. The resulting mass and radius are derived from the best-fitting model for the observed $\Delta\nu_0$, ν_{max} and known $T_{\rm eff}$, and [M/H]. This method is called as grid-based method (see [7] and references therein), which is not direct but assumes modelling.

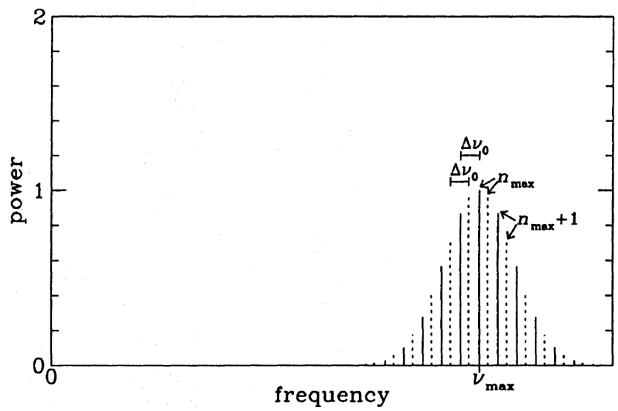

Fig. 2. Schematic diagram of the power spectrum of solar oscillations. Each peak corresponds to an oscillation mode: solid peaks are $\ell = 0$ modes and dashed peaks are $\ell = 1$. Copy of Fig.4 from [5].

Huber et al. [6] performed fundamental parameters determinations for 10 stars using simultaneously interferometric and asteroseismic observations provided by space missions *Kepler* or *CoRoT*. The authors provided detailed description of

the methods, performed a careful analysis of the possible errors and made comparisons between the parameters derived by different methods. They found that asteroseismic radii are accurate to 4 %. A comparison between asteroseismic and interferometric radii is shown in Fig.7 of [6], which is reproduced in Fig. 3. Other comparisons will be mentioned later.

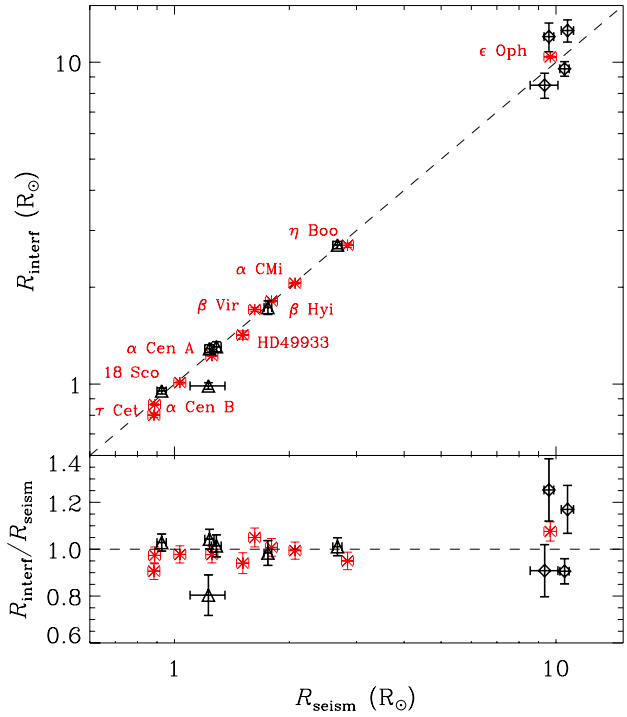

Fig. 3. Comparison of stellar radii measured using interferometry (PAVO) and calculated using asteroseismic scaling relations. Black diamonds show Kepler and CoRoT sample, and red asterisks show several bright stars as indicated in the plot for comparison. The dashed line marks the 1:1 relation. Copy of Fig.7 from [6]. See details in [6].

4. PHOTOMETRY

Now I briefly describe fundamental parameters determinations based on the photometric observations.

4.1. Infrared Flux Method (IRFM)

This method was proposed by [8] first to derive stellar radii. The main idea is that stellar angular diameter is defined by the ratio of the flux measured at the

top of Earth's atmosphere $f_{\rm bol}$ to the flux emitted from the stellar surface $F_{\rm bol}$, and this relation is valid for the bolometric fluxes and for any monochromatic flux (infrared, for example):

$$\theta^2_{\rm LD} = 4f_{\rm bol}/F_{\rm bol} = 4f_\lambda/F_\lambda \tag{3}$$

While $F_{\rm bol} = \sigma T^4_{\rm eff}$, we have a relation for $T_{\rm eff}$:

$$T_{\rm eff} = \left(4\frac{f_{\rm bol}}{\sigma}\frac{F_{\rm IR}}{f_{\rm IR}}\right)^{1/4} \tag{4}$$

Surface infrared monochromatic flux $F_{\rm IR}$ is chosen because for stars hotter than 4000 K it is dominated by the continuum opacities, which are rather well known, and it depends linearly on $T_{\rm eff}$ (Rayleigh–Jeans region). Hence, this flux is easily calculated from the model atmosphere. The bolometric flux $f_{\rm bol}$ is derived from the multi-band photometry taking into account the bolometric correction (see Fig 1). The IR flux $f_{\rm IR}$ is usually derived from JHKS magnitudes. Iterative procedure is used to determine $T_{\rm eff}$ because of the mild dependence of the bolometric corrections and IR fluxes on atmospheric model. After $T_{\rm eff}$ determination it is easy to derive stellar angular diameter and linear radius for the stars with known parallaxes. $R/R_\odot$ determinations. The homogeneous $T_{\rm eff}$ scale was obtained for more that 1000 dwarf and giant stars in the wide range of parameters: $3600 \leq T_{\rm eff} \leq 8000$ K and $-4.0 \leq [Fe/H] \leq +0.5$ ([9] and references therein). Based on these determinations Ramírez & Meléndez [10] provided metallicity-dependent temperature versus color calibrations. Calibration coefficients for seventeen colors in the photometric systems UBV, uvby, Vilnius, Geneva, RI(Cousins), DDO, Hipparcos-Tycho, and Two Micron All Sky Survey (2MASS) were derived which fit the IFRM $T_{\rm eff}$ with standard deviations from 30 to 120 K. Fig. 4 shows a comparison between angular diameters and effective temperatures derived by direct methods (interferometry) and by IRFM. These plots are taken from [9] (Figs.14,16).

No systematic shifts are noticeable. Angular diameters derived by two methods agree to better than 0.2 mas on average; effective temperatures agree within 70 K with the small shift of 18 K.

5. SPECTROSCOPY

Determination of the stellar atmosphere parameters by means of spectroscopy is based on the selective sensitivity of the line intensities and the line profiles to the variations of the atmospheric parameters: $T_{\rm eff}$, $\log g$, element abundance $\epsilon_{\rm el}$, and microturbulent velocity $\xi_{\rm t}$.

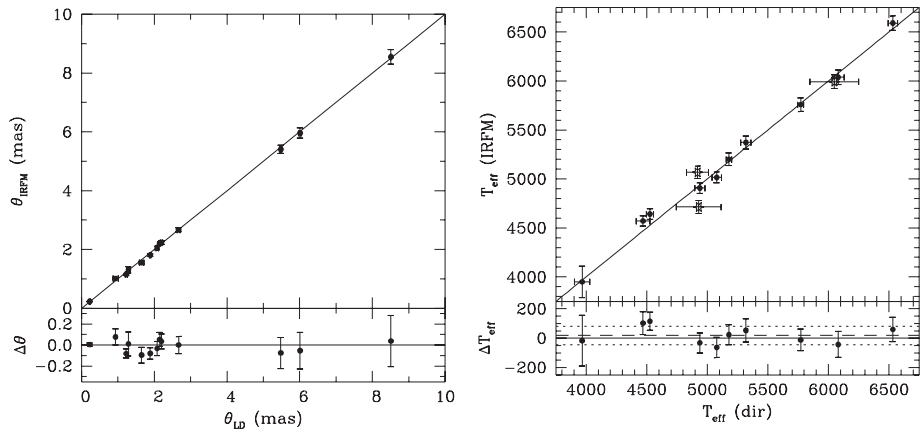

Fig. 4. Comparison of stellar angular diameters (left panel) and $T_{\rm eff}$ (riht panel) measured using interferometry ($\theta_{\rm LD}$, $T_{\rm eff}$ (dir)) and by IRFM ($\theta_{\rm IRFM}$, $T_{\rm eff}$ (IRFM)). Copy of Figs.14,16 from [9]. See details in [9].

5.1. Equivalent widths method

The eqiuvalent width (EqW) method is based on the EqW measurements of well-defined absorption lines. Usually, the lines of Fe I and Fe II are used because the stellar line spectrum consists of the numerous lines of this element with accurate atomic parameters for many of them. If one has a model atmosphere then it is easy to calculate theoretical line EqW and deduce the individual line abundances The final atmospheric parameters are derived by removing any dependance of individual line abundances on the excitation energy E.P. (excitation balance – $T_{\rm eff}$ indicator), on the line equivalent width ($\xi_{\rm t}$ indicator), and on the equal mean abundances for Fe I/Fe II lines (ionization balance – surface gravity indicator).

where

These three equilibrium conditions are solved simultaneously to derive the stellar atmospheric parameters: effective temperature ($T_{\rm eff}$), surface gravity ($\log g$), microturbulent velocity ($\xi_{\rm t}$), and the iron abundance ([Fe/H]). A good description of EqW method is given in [11] and is illustrated here by plots taken from this article (Fig. 5).

EqW method has been successfully applied to study large samples of F, G, and K solar type stars (see, for example [12, 13] – 1033 stars).

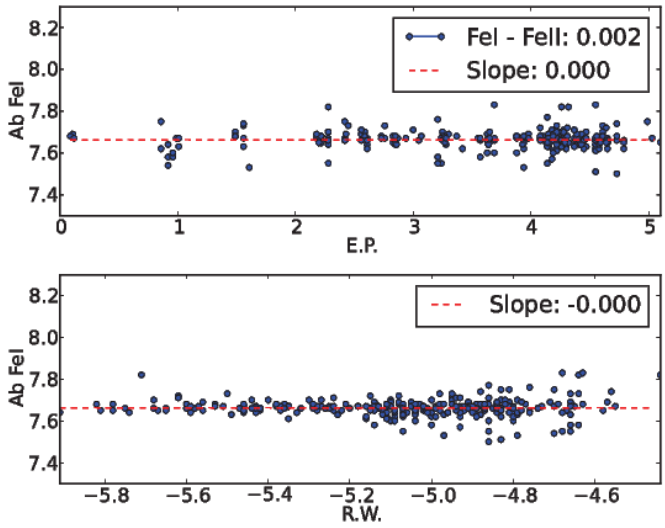

Fig. 5. Abundance of Fe I as a function of excitation potential (E.P.) and reduced equivalent width (R.W.) for the final stellar parameters of the solar-type star HD 1461 [11].

5.2. Spectrum fitting

The EqW method is mostly based on the lines of Fe I and Fe II because they compose the largest part of the lines with the accurate atomic parameters observed in stellar spectra. However, in hot stars Fe I lines disappeared from stellar spectra, while atomic parameters for higher ionization lines are not enough accurate and may produce large errors in atmospheric parameters determinations.

'Spectroscopy Made Easy' (SME) program package, developed by [14, 15] allows us to determine automatically the atmospheric parameters $T_{\rm eff}$, $\log\, g$, average metallicity [M/H], and also parameters of atmospheric velocity fields ($v_{\rm e} \sin i$, $\xi_{\rm t}$, $V_{\rm macro}$) by fitting the synthetic spectrum to the high-resolution, high signal-to-noise ratio stellar spectrum. SME solver consists of the IDL routines for preparing spectral synthesis and performing optimization, and external library for synthetic spectrum calculations. The external library (synth code) is written in C++ and Fortran. SME spectral synthesis consists of molecular and ionization equilibrium solver EOS, continuous opacity package CONTOP, line opacity package LINEOP and radiative transfer solver RTINT.

SME is working with the observations in ascii or fits formats. The format of the input linelist is the output format of VALD 'Extract Stellar' request ([16]). SME has model libraries of Kurucz' (1993) models [17], the latest version of MARCS models [18] and LLmodels set of models [19]. While in EqW method the lines of

Fe I and Fe II are mostly utilized, many spectral lines of different elements in first three ionization states are used simulteneously for parameters determination in SME. Current versions of SME include NLTE departure coefficients for MARCS and LLmodels sets [15,20].

The user constructs spectral mask where lines/regions for fitting procedure are marked. An example of SME mask is given in Fig. 6.

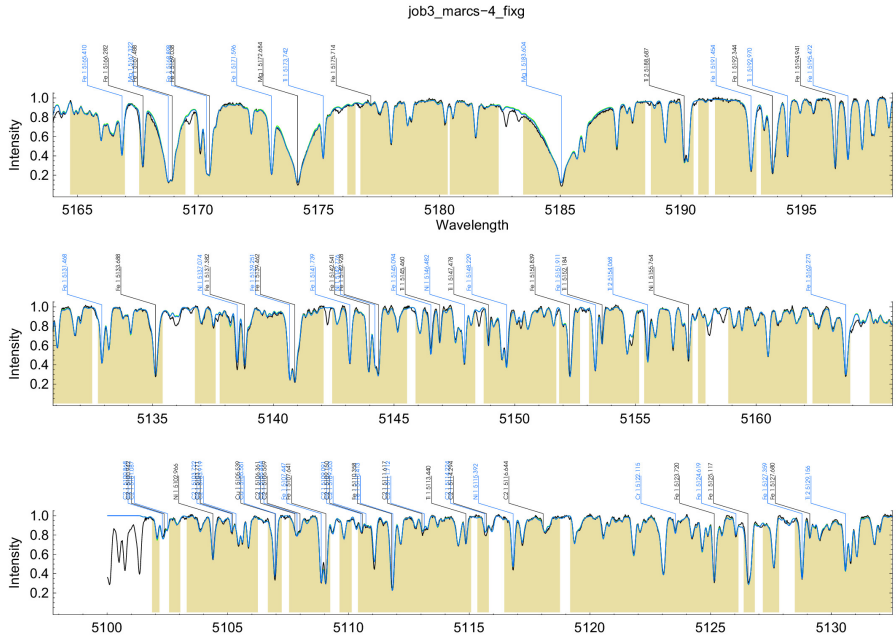

Fig. 6. An example of spectral mask in solar-type star HD 107211 for SME analysis. Observations are shown by black line, synthetic spectrum calculations are shown by blue line. The spectral regions participated in fitting are marked by yellow colour, those omitted from fitting are marked by white.

First, the user derives the global parameters. Once fixing atmospheric parameters: $T_{\rm eff}$, $\log g$, average metallicity [M/H], $v_{\rm e} \sin i$, $\xi_{\rm t}$, $V_{\rm macro}$, SME allows to perform a full abundance analysis.

SME was applied to parameter determination of 1617 planet-search FGK stars [21]. There are 98 common stars analysed by EqW ([12,13]) and SME methods. Comparison of the parameters derived by two spectroscopic methods, ionization equilibrium (EqW) and SME, is shown in Fig. 7 (top panels), while on the bottom panels a comparison between the parameters derived by SME and asteroseismology methods is displayed.

There is an evident trend for SME results to produce slightly higher $T_{\rm eff}$ and $\log g$, for stars hotter than 5500–6000 K. However, we may conclude that stel-

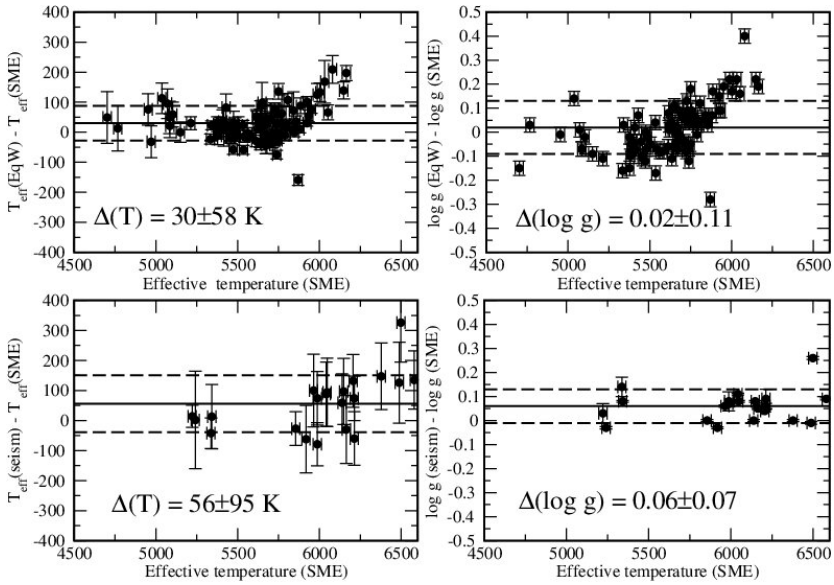

Fig. 7. Comparison of the $T_{\rm eff}$ and $\log g$ derived by ionization equilibrium (EqW) and profile fitting (SME) spectroscopic methods (top panels). The same is for comparison between SME and asteroseismology methods (bottom panels).

lar parameters $T_{\rm eff}$ and $\log g$ derived by different spectroscopic methods and by asteroseismology agree within 100 K and 0.1 dex.

6. CONCLUSION

Different methods of stellar fundamental parameters determination are considered. Comparison between these methods allow us to conclude that stellar angular diameters (linear radii) may be derived with the uncertainty better than 7%. Effective temperatures $T_{\rm eff}$ and surface gravities determinations agree within 100 K and 0.1 dex, respectively. These limits exceed the uncertainty estimates cited in different analyses of large star samples.

The current work was performed with the partial financial support from the Presidium RAS program KP19-270.

REFERENCES

1.

2. Boyajian Tabetha S., von Braun Kaspar, van Belle Gerard, et al., ApJ, 2013, **771**, 408.

3. Ligi R., Creevey O., Mourard D., et al., A&A, 2016, **586**, A94.

4. Gaia Collaboration, Brown A. G. A., Vallenari A., et al., A&A, 2018, **616**, A1.

5. Kjeldsen H. and Bedding T. R., A&A, 1995, **293**, 87

6. Huber D., Ireland M. J., Bedding T. R., et al., ApJ, 2012, **760**, 32.

7. Silva Aguirre V., Casagrande L., Basu S. et al., ApJ, 2012, **757**, 99

8. Blackwell D. E. and Shallis M. J., MNRAS, 1977, **180**, 177

9. Ramírez Iván and Meléndez Jorge, ApJ, 2005, **626**, 446

10. Ramírez Iván and Meléndez Jorge, ApJ, 2005, **626**, 465

11. Sousa Sérgio G., in Series: GeoPlanet: Earth and Planetary Sciences, 2014, Ewa Niemczura, Barry Smalley and Wojtek Pych eds., Springer International Publishing, Chambridge, 297

12. Sousa S. G., Santos N. C., Mayor M., et al., A&A, 2008, **487**, 373

13. Sousa S. G., Santos N. C., Israelian G., et al., A&A, 2011, **533**,

14. Valenti J. A. and Piskunov N., A&A Suppl., 1996, **118**, 595

15. Piskunov N. and Valenti J. A, A&A, 2017, **597**, A16

16. Ryabchikova T., Piskunov N., Kurucz R. L. et al., Phys. Scripta, 2015, **90**, 054005

17. Kurucz R., ATLAS9 Stellar Atmosphere Programs and 2 km/s grid. Kurucz CD-ROM No. 13. Cambridge, Mass.: Smithsonian Astrophysical Observatory, 1993., 13

18. Gustafsson B., Edvardsson B., Eriksson K. et al., A&A, 2008, **486**, 951

19. Shulyak D., Tsymbal V., Ryabchikova T. et al., A&A, 2004, **428**, 993 A141

20. Piskunov N., Ryabchikova T., Pakhomov Y. et al., ASPC, 2017, **510**, 509

21. Brewer John M., Fischer Debra A., Valenti Jeff A. and Piskunov Nikolai, ApJS, 2016, **225**, 32